Faraday waves on a viscoelastic liquid

C. Wagner[1], H. W. Müller[2,3], and K. Knorr[1]

[1] *Institut für Technische Physik , Universität des Saarlandes Postfach 151150, D-66041 Saarbrücken, Germany*
[2] *Institut für Theoretische Physik, Universität des Saarlandes Postfach 151150, D-66041 Saarbrücken, Germany*
[3] *Max Planck Institut für Polymerphysik, Ackermannweg 10, D-55128 Mainz*

We investigate Faraday waves on a viscoelastic liquid. Onset measurements and a nonlinear phase diagram for the selected patterns are presented. By virtue of the elasticity of the material a surface resonance synchronous to the external drive competes with the usual subharmonic Faraday instability. Close to the bicriticality the nonlinear wave interaction gives rise to a variety of novel surface states: Localised patches of hexagons, hexagonal superlattices, coexistence of hexagons and lines. Theoretical stability calculations and qualitative resonance arguments support the experimental observations.

PACS: 47.50.+d 47.54.+r 47.20.Ma

The generation of standing waves on the surface of a vertically vibrated Newtonian fluid (Faraday waves) is one of the classical hydrodynamic pattern forming instabilities [1]. Theoretical and experimental investigations during the last decade have substantially improved our understanding of the underlying processes [2]. Recently pattern formation in viscoelastic fluids came into the focus of nonlinear science, too. The memory of viscoelastic fluids introduces an additional time scale, which gives rise to a number of interesting phenomena [3–7]. It is amazing that already Faraday [1] tried to compare Newtonian fluids with viscoelastic ones: *"The difference between oil and white of egg is remarkable; (...) the crispated state may be a useful and even important indication of the internal constitution of different fluids."* In Newtonian fluids the prevailing surface mode of the Faraday experiment is usually subharmonic (S), i.e. the waves oscillate with twice the period of the external excitation. Nevertheless, for very thin layers the surface oscillation may become harmonic (H), i.e. synchronous to the external drive [8,9]. However, the necessary vibration conditions are rather extreme, rendering this parameter region difficult to explore.

On the other hand, viscoelastic Maxwell fluids have recently been predicted to exhibit the harmonic Faraday resonance [10], if the external drive frequency compares to the elastic relaxation time of the fluid. This statement is based on the elasticity of the material and independent of the filling level. Thus selecting a polymeric liquid with an appropriate elastic time scale will open a new way to a systematic investigation of the harmonic Faraday instability. The present paper deals with such an experiment. The predicted harmonic resonance competes with the usual subharmonic instability. Close to the bicritical-ity an interesting new surface dynamics occurs, unknown in Newtonian fluids.

Our working fluid is a 1.5% (by weight) solution of PAA (polyacrylamide-co-acrylic acid of molecular weight 5×10^6, Aldrich 18,127-7) in a 60 : 40 glycerol-water solvent. The tabulated values for density, surface tension and dynamic viscosity of the *solvent* at $20°C$ are $\rho = 1,154kg/m^3$, $\sigma = 0.069N/m$ and $\eta = 11mPas$. For the polymeric solution the complex dynamic viscosity $\eta^\star(f) = \eta'(f) - i\eta''(f)$ has been measured at room temperature ($\simeq 22°C$) with a rotational viscometer (Rheometrics Fluids). Data acquisition for frequencies above $f = 16Hz$ was not possible. However, within the range $1Hz < f < 16Hz$ the data could well be fitted by the following power laws: $\eta' = 0.082 \times f^{-0.594}Pas$ and $\eta'' = 0.122 \times f^{-0.549}Pas$, where f is measured in Hz. These relations have been used to extrapolate the viscosity data into the frequency range of our experiment ($30Hz < f < 100Hz$).

The experimental setup consist of a black container built out of anodised aluminium with an inner diameter of 290 mm, filled to a height of 3 mm with the working fluid. By means of an electromagnetic shaker (V617 Gearing & Watson) the container is vibrated vertically with an acceleration $a \cos \Omega t$, where $\Omega = 2\pi f$. The container is covered and sealed by a glass plate to prevent evaporation and pollution. No degradation or drift of the experimental results could be detected within a period of four weeks. Due to the heat production of the vibrator we were not able to work at room temperature, where the rheometric viscosity data have been taken. A heat wire filament regulates the temperature at $30°C \pm 0.1$, measured by a PTC-resistor imbeded in the bottom of the vessel. Waveform generation as well as data acquisition are performed by a D/A-board (National Instruments, AT-MIO 16 E2) in a Pentium PC. The vibration signal measured by a piezoelectric device (Bruel & Kjear 4393) was checked to be sinusoidal with contributions from higher harmonics not more than 2%. A ring of 150 LED's with twice the container diameter is mounted on the vertical axis of the setup and illuminates the surface. The light reflected into the centre of the ring is recorded by a full frame CCD camera (Hitachi KPF-1). Its electronic shutter allows to synchronise the exposure with the external drive signal an thus to discriminate the H and S surface response. The phase diagram of the selected patterns is obtained by quasi-statically ramping the drive amplitude from just below the onset $\epsilon = \frac{a}{a_c} - 1 = -5\%$
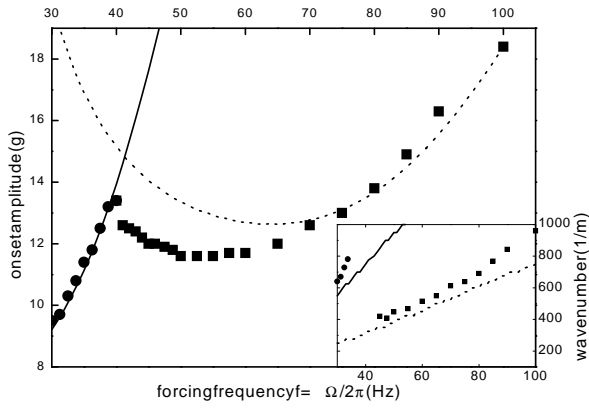
FIG. 1. The acceleration amplitude a_c and critical wave numbers k_H and k_S for the onset of the harmonic (circles) and subharmonic (squares) Faraday instability. Experimental data are plotted by symbols, lines denote the theoretical computation on the basis of the rheometric viscosity data $\eta^\star(f)$.

up to $\epsilon = 10\%$ while keeping the frequency constant. During each scan the amplitude is increased by 1%-steps and held constant for 300 seconds in between. Then, the surface of the fluid is photographed and the time dependence of the surface oscillation (whether S or H) is determined. Similar downwards-amplitude scans are performed to detect a possible hysteresis.

Fig. 1 shows the threshold amplitude a_c for the critical wave numbers of the Faraday instability. In the frequency domain above $f \simeq 60 Hz$ one observes the usual subharmonic Faraday resonance with a surface pattern of lines. Since this behavior is similar to high viscosity Newtonian liquids [11,12], we denote this region as the Newtonian regime. The present paper, however, is focused on the frequency range below $40 Hz$, where the surface responds harmonically. The predominance of the harmonic Faraday resonance has recently been predicted for viscoelastic Maxwell fluids [10]. On using the rheometric viscosity data for our working fluid we have computed the stability threshold (lines in Fig. 1) by the method of Kumar and Tuckerman [13]. Favourable agreement is achieved except for frequencies close to the bicritical intersection point. There are two possible sources for discrepancies: (i) There is a $7 - 9°C$ difference between the temperature of our experimental setup and that of the rheometer during the viscosity measurement. (ii) Errors due to the extrapolation of the viscometric data into the frequency range of our experiment.

Fig. 2 depicts the phase diagram of the selected patterns. The surface structure in region IIa is a uniform pattern of hexagons covering the whole surface, while in IIb we observe very stable localised patches of hexagons (see Fig. 3a). A slight onset hysteresis up to 6% in ε is visible. The pattern selection processes for
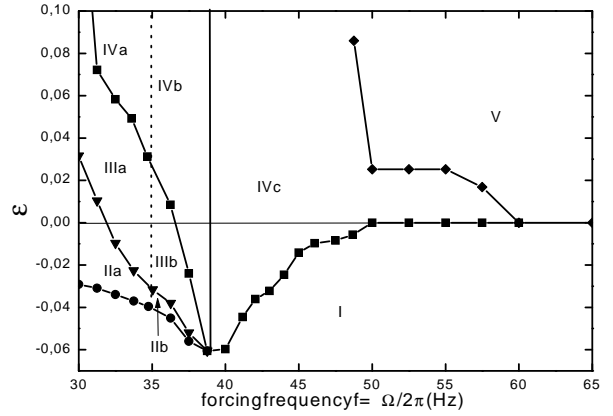
FIG. 2. Phase diagram of the observed nonlinear patterns. The symbols mark experimental data points. The abscissa, $\varepsilon = 0$, indicates the linear threshold shown in Fig. 1. The lowest solid line denotes the saddle point of the hysteresis. Region I: flat surface; IIa: harmonic hexagons covering the whole surface; $IIIa$: harmonic-subharmonic hexagonal super-lattice (see text) extending over the whole surface; $IIb, IIIb$: as before but *localised patches* surrounded by the flat surface; IVa, IVb, IVc: chaotic dynamics of subharmonic lines competing with extended (a) or localised (b) hexagonal superlattices or the flat surface (c); V: stationary subharmonic lines extending over the whole surface (Newtonian regime).

the backwards bifurcating hexagons in the harmonic region II and the forwards bifurcating lines in the subharmonic Newtonian regime V rely on the distinct respective time dependencies. This can be seen as follows: On taking the surface elevation η as a representative order parameter one has

$$\eta(\mathbf{r}, t) = \left[\sum_m \left\{ \begin{array}{c} H_m e^{i\mathbf{k}_{Hm} \cdot \mathbf{r}} \\ S_m e^{i\mathbf{k}_{Sm} \cdot \mathbf{r}} \end{array} \right\} + c.c. \right] \times \quad (1)$$

$$\sum_{n=-\infty}^{+\infty} \eta_n \left\{ \begin{array}{c} e^{in\Omega t} \\ e^{i(n+\frac{1}{2})\Omega t} \end{array} \right\} \quad \text{for} \quad \left\{ \begin{array}{c} H \\ S \end{array} \right\}.$$

Here $\mathbf{r} = (x, y)$ is the horizontal coordinate, the lateral wave vectors $\mathbf{k}_{Hm}$ and $\mathbf{k}_{Sm}$ with $|\mathbf{k}_{Hm}| = k_H$ and $|\mathbf{k}_{Sm}| = k_S$ compose the spatial pattern and the η_n are the temporal Fourier coefficients determined by the linear stability problem (components of the Floquet eigenvector). A similar ansatz holds for the velocity field $\mathbf{v}$. On feeding η and $\mathbf{v}$ into an arbitrary quadratic nonlinearity of the hydrodynamic equations results in a frequency spectrum of integral multiples of Ω, no matter whether S or H is considered. Thus quadratic nonlinearities are able to resonate with *harmonic* linear eigenmodes, but not with *subharmonic* ones. Clearly, spatial resonance must be granted as well. Thus any triple of harmonic modes $\{\mathbf{k}_{H1}, \mathbf{k}_{H2}, \mathbf{k}_{H3}\}$ with $|\mathbf{k}_{Hm}| = k_H$ and $\mathbf{k}_{H1} + \mathbf{k}_{H2} + \mathbf{k}_{H3} = 0$ is in resonance. This generic 3-wave vector coupling is well known e.g. from Non-Boussinesq-Rayleigh-Bénard convection and enforces a saddle node
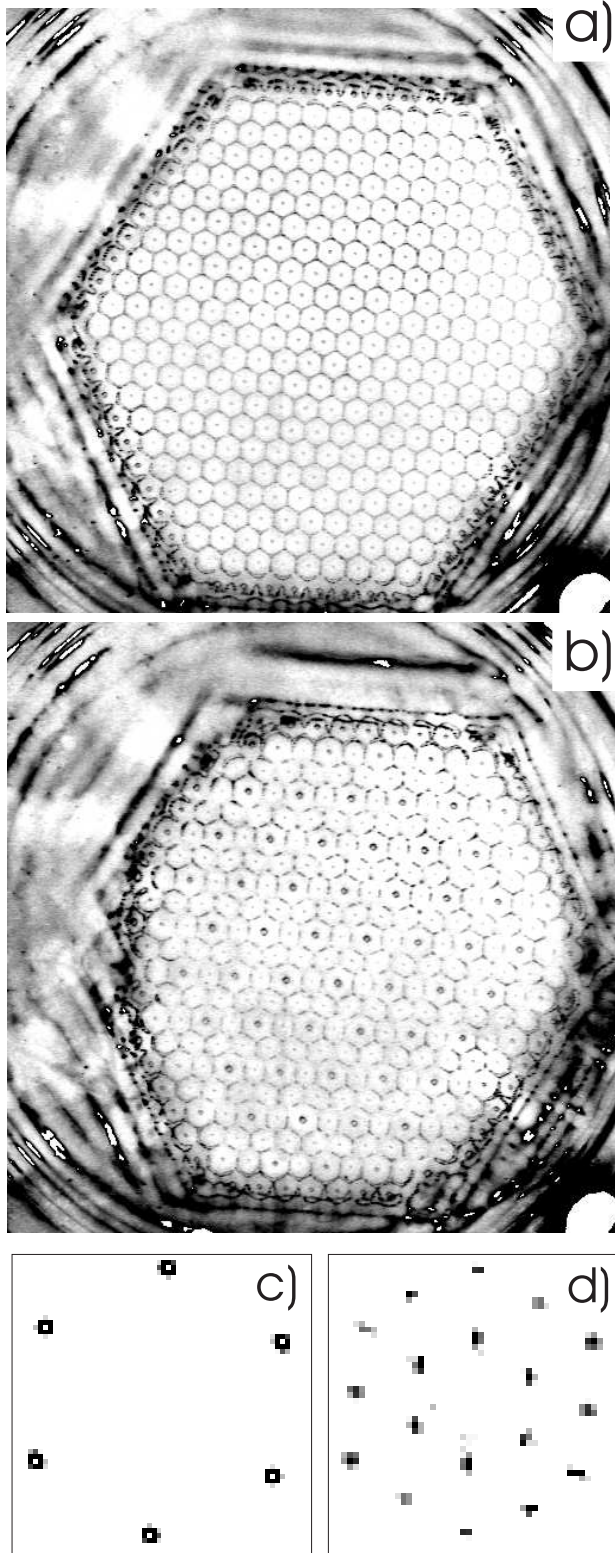
FIG. 3. Localised stationary surface patterns of harmonic hexagons (a) and the harmonic-subharmonic hexagonal superlattice (b) as observed in region IIb and $IIIb$ at $f = 37Hz$ and $\varepsilon = -0.05$ and -0.03. The corners of the picture show the outer edge of the container. In (c) and (d) the respective spatial Fourier spectra are shown. Patterns in regions IIa and $IIIa$ are similar but they cover the whole surface.

bifurcation towards hexagonal patterns. The associated amplitude equations are of the form (use cyclic permutation to get the other ones; κ and γ are nonlinear coefficients)

$$\partial_t H_1 = \varepsilon H_1 + \kappa H_2^\star H_3^\star - \left\{ |H_1|^2 + \gamma \left[|H_2|^2 + |H_3|^2 \right] \right\} H_1. \tag{2}$$

Within the Newtonian region V such a resonant 3-wave vector coupling is prohibited due to the missing temporal resonance. Quadratic nonlinearities in the evolution equations for the S_m are prohibited and the pattern selection mechanism is controlled by the cubic nonlinearity [14,12]. It is instructive to point out that the subharmonic *temporal* symmetry $\eta(t + 2\pi/\Omega) = -\eta(t)$ for Faraday waves is analogous to the *spatial* up-down symmetry for Rayleigh-Bénard convection (known as the Boussinesq symmetry): They both prevent quadratic nonlinearities to appear in the associated amplitude equations.

If the drive amplitude is raised from IIa, b to $IIIa, b$, a sharp secondary transition can be detected: Subharmonic frequency contributions suddenly appear in the temporal Fourier spectrum of the surface elevation. Simultaneously the associated spatial Fourier spectrum (Fig. 3c,d) exhibits a hexagonal superstructure with the same orientation but a wavelength twice as long as the primary one. The theoretical stability calculation indicates that the *primary* subharmonic onset (dashed line in Fig. 1) is situated far above the $II - III$ transition. Therefore, the secondary superstructure has to result from a nonlinear excitation process. The underlying mechanism is again a 3-wave vector interaction: Invoking basic resonance arguments the subharmonic mode $\mathbf{k}_{S1} = \frac{1}{2}\mathbf{k}_{H1}$ with amplitude S_1 obeys the following amplitude equation (use again cyclic permutation to get the equations for S_2 and S_3)

$$\partial_t S_1 = -\lambda S_1 + \chi H_1 S_1^\star + \text{higher order terms}. \tag{3}$$

Here $\lambda > 0$ reflects the linear damping and χ is a nonlinear coupling coefficient. According to Eq. (3) the secondary crossover from II to III occurs when the primary pattern amplitude $|H_m| = H$ exceeds the threshold $\lambda/|\chi|$.

The dashed lines in Fig. 2 separating the subregions of homogeneous (a) and localised (b) hexagons are to be considered as approximate boundaries rather than sharp transition lines. On increasing f, the localised patches decrease in size until they dissappear at $f > 39Hz$. However, on keeping f fixed their size is rather robust and hardly depends on the forcing amplitude a. Note that these new localised patches of hexagons cannot be explained by a set of Ginsburg-Landau equations, which supplements Eqs. (2) by diffusive spatial derivatives: Within this familiar model isolated islands of hexagons do not *stably* exist over a finite control parameter interval.
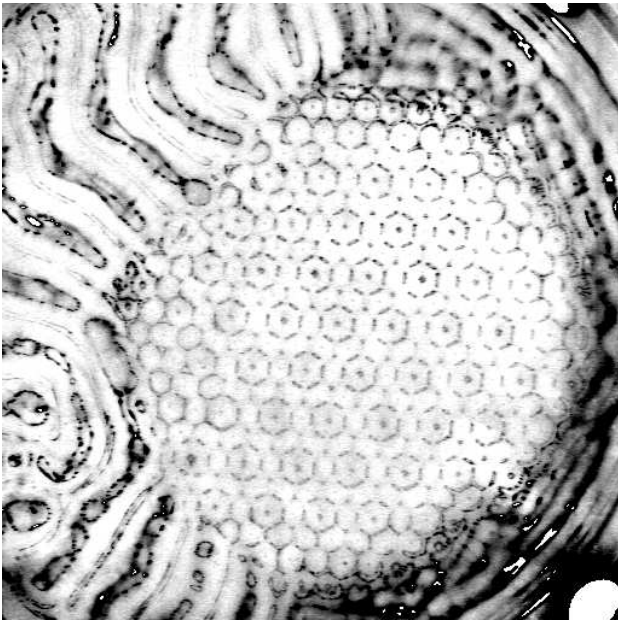
FIG. 4. Snapshot of a time dependent surface state in region IVb at $f = 37Hz$ and $\varepsilon = 2$. A stationary localised patch of hexagons is surrounded and competes with subharmonic lines moving in an erratic manner across the surface.

On entering region IVa or IVb the patterns become chaotically time dependent. Patches of subharmonically oscillating lines originating in an erratic manner from the cell boundary (a) or respectively from the flat surface (b) penetrate into the stationary hexagonal superlattice. Then they disappear again and the original structure is recovered. This dynamics repeats on time scales of the order of seconds to minutes, leading to a temporary co-existence of the stationary hexagonal superlattice with subharmonic lines (see Fig. 4). Higher drive amplitudes lead to a fully chaotic surface pattern.

For drive frequencies in the intermediate region Vc a similar chaotic behavior of subharmonic lines can be observed, however directly as the *primary* instability. Since hexagons do not occur beyond $f \simeq 39Hz$, the subharmonic lines compete with the flat surface state. Nevertheless, the bifurcation still exhibits a small hysteresis, which continuously goes down as f approaches $60Hz$.

In summary, we have presented experimental results on Faraday waves in a viscoelastic medium. Earlier theoretical predictions of the harmonic Faraday resonance could be confirmed. Our measurements are the first systematic study of harmonic Faraday waves, which could not be performed yet for Newtonian fluids. The empiric onset data are found in good quantitative agreement with the theory. Furthermore the appearance of uniform hexagonal patterns and their (secondary) transition towards a harmonic-subharmonic superlattice is understood in terms of elementary $3-$wave vector resonances. Besides spatially homogeneous wave patterns we find very robust and sharply localised patches, which are surrounded by the flat surface or – at higher drive amplitudes – in com-plicated dynamical competition with subharmonic lines. Their explanation requires a more elaborate theory.

[1] M. Faraday, Philos. Trans. R. Soc. London **52**, 319 (1831).
[2] for a review see: J. W. Miles and D. Henderson, Ann. Rev. Fluid Mech. **22**, 143 (1990); H. W. Müller, R. Friedrich, and D. Papathanassiou, *Theoretical and experimental studies of the Faraday instability*, in: *Lecture notes in Physics*, ed. by F. Busse and S. C. Müller, Springer (1998).
[3] C. M. Vest and V. S. Arpaci, J. Fluid Mech. **36**, 613 (1969); M. Sokolov and R. I. Tanner, Phys. Fluids **15**, 534 (1972).
[4] H. R. Brand and B. J. A. Zielinska, Phys. Rev. Lett. **57**, 3167 (1986); B. J. A. Zielinska, D. Mukamel and V. Steinberg, Phys. Rev. E **33**, 1454 (1986).
[5] H. Pleiner, J. L. Harden and P. Pincus, Europhys. Lett. **7**, 383 (1988).
[6] R. G. Larson, E. S. Shaqfeh, and S. J. Muller, J. Fluid Mech. **218**, 537 (1990); R. G. Larson, Rheol. Acta **31** , 213 (1992).
[7] A. Groisman and V. Steinberg, Phys. Rev. Lett. **77**, 1480 (1996); **78**, 1460 (1997); Europhys. Lett. **43**, 165 (1998).
[8] E. Cerda and E. Tirapegui, Phys. Rev. Lett. **78**, 859 (1997); J. Fluid Mech. **368**, 195 (1998).
[9] H. W. Müller, H. Wittmer, C. Wagner, J. Albers, and K. Knorr, Phys. Rev. Lett. **78**, 2357 (1997).
[10] H. W. Müller and W. Zimmermann, to appear in Europhys. Lett. (1998).
[11] W. S. Edwards and S. Fauve, J. Fluid Mech. , **278**, 123 (1994).
[12] P. Chen and J. Vinals, Phys. Rev. Lett. **79**, 2670 (1997).
[13] K. Kumar and L. S. Tuckerman, J. Fluid Mech. **279**, 49 (1994).
[14] H. W. Müller, Phys. Rev. Lett. **71**, 3287 (1993).